Thermal–Mechanical Fatigue Behaviour of Nickel Base Superalloy Single Crystals

E. FLEURY and L. REMY
Centre des Matériaux de l'Ecole des Mines de Paris, URA CNRS DO250, BP 87, 91003 Evry Cedex, France

ABSTRACT

Thermal-mechanical fatigue tests as well as isothermal low cycle fatigue tests were carried out on single crystals of a nickel-base superalloy, AM1, to investigate the stress-strain behaviour and fatigue damage under anisothermal conditions. The present paper reports results for the [001] direction. A mechanical strain-temperature loop was used from 600° to 1100°C (873 to 1373K) with peak strains at intermediate temperatures. Thermal mechanical fatigue (TMF) cycling was observe to cause less cyclic hardening than isothermal low cycle fatigue (LCF) experiments at temperatures where mechanical strain was maximum or minimum. Fatigue life to crack initiation under TMF cycling was found to be intermediate between the LCF lives at the peak strain temperatures. The TMF life to initiate a 50μm deep crack can be deduced from these LCF data using a simple relationship.

KEYWORDS

Thermal-mechanical fatigue, nickel-base superalloy, monocrystalline, fatigue damage, crack initiation.

INTRODUCTION

Many engineering components operating at elevated temperatures are submitted to thermal fatigue due to start-up and shut-down operations. This is especially the case of turbine blades in jet engines. For a long time the resistance to thermal fatigue of candidate materials has been assessed using Glenny-type tests or wedge type specimens in a burner rig (Rémy, 1987). In these tests the thermal stress arises from transient temperature differences between various points of the test specimen, and stress and strain have to be derived from a finite element analysis as for a real component. Thermal-mechanical fatigue tests (TMF) were introduced to simulate the behaviour of critical parts of components (Hopkins, 1976). There is no temperature gradient across the specimen section and the stress is induced by a mechanical strain to simulate the constrained free thermal expansion of a component part (which is due to temperature gradients across the component section). Since temperature, stress and strain are directly

measured, TMF tests can be used to check predictions of stress-strain behaviour models as well as of damage models.
The design of advanced jet engines with improved performances has led to the development of blades made from directionaly solidified single crystals. Such components show higher creep rupture life as well as longer thermal fatigue life than conventionaly cast superalloys (Boone and Sullivan, 1973). The marked improvement in thermal fatigue resistance is mainly due to the fact that the [001] solidification direction of the blades corresponds to the minimum value of Young's modulus, which reduces the thermal stress (Gemma *et al.*, 1976).
Therefore the thermal-mechanical fatigue behaviour of single crystals of a nickel base superalloy, AM1, was investigated to identify the mechanisms of fatigue failure under thermal stress cycling. Both the cyclic stress-strain behaviour and the fatigue life were studied using a temperature variation between 600°C and 1100°C and a cycle where strain and temperature were not in phase. The life to crack initiation was especially studied using plastic replicas and was compared with isothermal low cycle fatigue (LCF) data at peak strain temperatures.

MATERIALS AND EXPERIMENTAL PROCEDURES

The nickel-base superalloy AM1 used in this investigation had the following chemical composition (in wt pct) : 6.5Co - 7.7Cr - 1.9Mo - 5.7W - 5.2Al - 5.9Ta - bal.Ni. Single crystals were in form of cast round bars 20 mm in diameter and 120 mm in length with their axis along a [001] direction. The single crystals bars were given a solution heat treatment at 1300°C for 3 hours, a precipitation heat treatment at 1100°C for 10 hours and a final aging heat treatment at 870°C for 16 hours. The microstructure was constituted by a distribution of γ' precipitates in a γ matrix. The size and volume fraction of γ' precipitates were approximately 0,40μm and 68pct, respectively.
To obtain a uniform temperature distribution in the radial direction, hollow cylindrical fatigue specimens were machined from the bars which had a 1 mm wall thickness. The dimensions of the gauge length and of the external diameter were 25 mm and 11 mm, respectively. Specimens were internally polished and the external surface was polished down to 3μm diamond paste.
The crystallographic orientation of specimens was checked using the Laue back reflexion X-ray diffraction technique. All specimens were within 7 degrees of the exact orientation.
Our own TMF test facility used a microcomputer to generate two synchronous temperature and mechanical strain signals (Malpertu and Rémy, 1988). The closed loop control was ensured for each signal by a temperature controller and by the testing machine, respectively. The imposed total strain range εt is the sum of the mechanical strain εm (which simulates the thermal loading of a part of a component) and the thermal strain εth. The free thermal expansion on heating and contraction on cooling is memorized by the computer and the mechanical strain can be chosen at will. Radiation heating was used and no forced cooling was allowed since it was necessary to have a negligible temperature difference across the specimen thickness to ensure that the test was representative of the behaviour of a volume element. Longitudinal strain control was ensured using a strain gauge extensometer with alumina knives in contact with the specimen.
A basic standard cycle was used to simulate blade behaviour which is shown in Fig. 1. A typical cycle involves temperature variation from 600° to 1100°C for a 3.5 min period. Thus minimum and maximum strains occur at intermediate temperature in this type of cycle (compression peak at 950°C during heating and tension peak at 700°C during cooling).
This cycle shows a diamond shape with a large hysteresis in a temperature-mechanical strain diagram. This shape is very similar to

published computations of Glenny's tapered discs (Glenny, 1974) or of wedge type specimens (Rezai-Aria *et al.*, 1983) submitted to thermal fatigue.

RESULTS AND DISCUSSION

Cyclic stress-strain behaviour

Cyclic stress-strain curves were mainly measured using single specimens which were submitted to increasing mechanical strain ranges. Figure 2 shows the variation of stress as a function of plastic strain for three mechanical strain ranges. Cyclic stress-mechanical strain loops were recorded using a computer which memorized thousand points per cycle and the plastic strain $\varepsilon p(t)$ was determined by the expression :

$$\varepsilon_p(t) = \varepsilon_m(t) - \frac{\sigma(t)}{E(t)} \qquad (1)$$

where $\varepsilon m(t)$, $\sigma(t)$ and $E(t)$ are the instantaneous total mechanical strain, stress and Young's modulus, respectively.
For this type of test and for this material, stress-strain loops are stabilized after a few cycles. Let us consider the strain-stress loops observed for a mechanical strain range of 2.6 pct for instance. Heating starts from 600°C at zero mechanical strain, decreases linearly and the stress become more compressive down to a minimum at 950°C. Then the mechanical strain increases to zero while the temperature reaches the maximum value of 1100°C. On cooling the stress becomes tensile up to a maximum at 700°C as the mechanical strain. Then the stress decreases down to a compressive value at minimum temperature (600°C) when the mechanical strain decreases to zero.
With this type of test where temperature is changing continuously, the compression peak stress did not correspond necessarily with the minimum mechanical strain. Stress in compression was minimum for a temperature below 950°C, and generaly plastic strain was minimum at 1040°C about. These phenomena show the complexity of the non-isothermal fatigue; the shape of the stress-strain hysteresis loop depends on the temperature variation of the Young's modulus, flow stress and of the kinetics of temperature variation.
Though strain cycling was fully reversed, the stress cycle was unbalanced : a positive tensile mean stress was observed for this cycle. The values of σmax , σmin are plotted against the half mechanical strain range ($\Delta\varepsilon m/2$) to obtain the cyclic stress-strain curves (CSS) under TMF cycling. These curves are shown in Fig. 3 along with the isothermal CSS curves obtained at 650°C and 950°C. At higher $\Delta\varepsilon m/2$ the maximum stress for TMF cycling is lower than for isothermal fatigue for both temperatures which show the loading path dependence of the stress-strain behaviour.
On Fig. 3, the evolution of σmax of isothermal cycling at 650°C shows an unstable increase of plastic strain above a critical plastic strain. Observation of TMF specimens has shown multiple slip on {111} planes (Fig. 4) like LCF specimens at 650°C. The oxide scale on the surface of TMF specimens shows microcracks perpendicular to the stress axis. Thus TMF specimens display direct evidence that low and high temperature mechanisms are superimposed : low temperature plastic deformation mechanisms and high temperature oxide scale damage mechanisms.

Thermal-mechanical fatigue life to crack initiation

TMF testing can be used to estimate the life of a critical part of component operating under thermal fatigue. Smooth specimen testing is

especially appropriate to investigate the life to engineering crack initiation (up to a crack depth smaller than 1 mm).
The development of microcracks was monitored in all the specimens using inspection of cellulose acetate replicas of specimen surface. The replication technique necessitates test interruptions at regular intervals but it enables cracks as small as 10 - 20μm in length to be detected. So we used two definitions of fatigue life. A first conventional fatigue life was defined to 0.3 mm crack depth, referred to as Ni. A second crack initiation criterion was defined at 50μm crack depth referred to as Na. As discussed in a previous work on IN100 cast superalloy (Malpertu and Rémy, 1988), this criterion should provide a much better description of crack initiation than the Ni criterion which can encompass a large part of microcrack propagation.
The aspect ratio (crack depth ap over width as) was investigated using observations of fracture surfaces. Results thus obtained are similar to LCF data on other superalloy single crystals (Bois, 1985). Cracks have a semi-elliptical shape keeping a constant aspect ratio : ap = 0.38.as
Many models consider thermal fatigue damage to be mainly due to fatigue (Coffin, 1973; Taira, 1973) or to some creep-fatigue interactions (Manson, 1973). Taira among others (Taira, 1973) tried to define an equivalent LCF temperature. Therefore the comparison between the resistance to thermal fatigue or thermal-mechanical fatigue and that to LCF was investigated by many authors (Halford and Manson, 1976; Sehitoglu and Karasek, 1986; Engberg and Larson, 1984).
LCF tests were thus carried out in order to make a comparison with TMF results. Tests were made at, or near the temperature of the peak mechanical strain i.e. 650°C (instead of 700°C for the tensile peak strain) and 950°C. TMF as well as LCF results are plotted versus the total mechanical strain range in Fig. 5. The TMF life to initiate a 50μm deep crack Na is much smaller than the life to 0.3 mm crack depth Ni. This means that the life to engineering crack initiation is mostly spent in crack growth. TMF results do not seem to fit a smooth curve as LCF data do. The breakdown in slope at high mechanical strain ranges could be linked with the breakdown in the cyclic stress-mechanical strain curves near $\Delta\varepsilon m = 1{,}5\%$ (Fig. 3). Comparison between TMF and LCF shows that TMF life to crack initiation is longer than LCF life at the temperature of the compressive peak strain and shorter than LCF at the temperature of a tensile peak strain.
Plastic strain range - TMF life curves can be fitted in log-log coordinates by straight lines within the experimental accuracy (Fig. 6). TMF curves seem to cross over LCF curves at 950°C while inelastic strains are almost negligible at 650°C and curves cannot be drawn for this temperature.
The comparison between LCF and TMF is more straightforward using a stress range life diagram (Fig. 7). The TMF life is almost twice the LCF life at 950°C and is much smaller than at 650°C.
One may assume as usually that damage accumulates in a linear way during the crack initiation period. The life to crack initiation could thus be approximated as the harmonic mean of initiation periods at the temperature of the peak strain in tension and in compression, respectively :

$$\frac{2}{Na_{,TMF}} = \frac{1}{Na[T(\varepsilon_{mmax})]} + \frac{1}{Na[T(\varepsilon_{mmin})]} \qquad (2)$$

Na[T(εmmin)] was simply deduced from replica measurements at 950°C. Na[T(εmmax)] was deduced from fatigue life Ni at 650°C assuming a constant crack growth rate throughout the test. The predicted life to crack initiation is reported as a solid line in Fig. 7 and is actually in pretty good agreement with TMF results. The TMF life to crack initiation is dominated by the mechanical strain peak at high temperature (compressive in the cycle used) for the present alloy. This result is borne out by

metallographic observations : the same morphology of microcracks in the oxide scale was observed in TMF specimens and in LCF specimens which were cycled at 950°C.

CONCLUSIONS

This investigation of the thermal-mechanical fatigue (TMF) behaviour of nickel-base superalloy single crystals enabled comparisons to be made with isothermal fatigue (LCF) at the temperature where the mechanical strain was maximum or minimum. Differences in cyclic stress-strain behaviour were observed between TMF and LCF at the temperature of the peak strains due the importance of the time-temperature-strain history.
Fatigue life to crack initiation under TMF cycling was found to be intermediate between the LCF lives at the peak strain temperatures. The TMF life to initiate a 50μm deep crack can be deduced from these LCF data using a simple relationship.

ACKNOWLEDGEMENTS

Single crystals were supplied by the Société Nationale d'Etudes et de Construction de Moteurs d'Aviation (SNECMA). The authors are indebted to the Direction des Recherches, Etudes et Techniques (DRET) of the french Ministery of Defence for the financial support of this work.

REFERENCES

Bill R., (1986). Fatigue at high temperature, Proc. Journées Internationales de Printemps, SFM, Paris, 9-11 June, pp.345-358.
Bois F., (1985). Thesis, Ecole des Mines de Paris, France.
Boone D.H. and Sullivan C.P., (1973). Fatigue at Elevated Temperatures, ASTM STP 520, American Society for Testing and Materials, pp.401-425.
Coffin L.F., (1973). Fatigue at elevated temperatures, ASTM STP 520, American Society for Testing and Materials, pp.5-34.
Engberg G. and Larsson L., (1984). Thermomechanical and low cycle fatigue of advanced nickel base alloys, COST 50 round 3, project S-3, final report, Swedish Institute for Metals Research.
Gemma A.E., Langer B.S. and Leverant G.R., (1976). Thermal Fatigue of Materials and Components, ASTM STP 612, pp.199-213.
Glenny R.J.E., (1974). High temperature materials in gas turbines, P.R. Sahm and M.O. Speidel, Eds., Elsevier, Amsterdam, pp.258-277.
Halford G.R. and Manson S.S., (1976). Thermal Fatigue of Materials and Components, ASTM STP 612, pp.239-254.
Hopkins S.W., (1976). Thermal fatigue of materials and components, ASTM STP 612, pp.157-169.
Malpertu J.L. and Rémy L., (1988). "Thermomechanical Fatigue Behaviour of a Superalloy", Low Cycle Fatigue, ASTM STP 942, pp.657-671.
Manson S.S., (1973). Fatigue at Elevated Temperatures, ASTM STP 520, American Society for Testing Materials, pp.744-782.
Rémy L., (1987). "Recent Developments in Thermal Fatigue" in high temperature fracture mechanics, proc. of an int. seminar Dourdan, France, 13-15 October, P. Bensussan etal. Eds, Mecamat, pp.IV.1 - IV.20.
Rezai-Aria F., Rémy L., Herman C. and Dambrine B., (1983). Mechanical Behaviour of Solid - IV, proc. 4th conf., Stockholm, Sweden, 15-19 aug., J. Carlsson and N.G. Ohlson, Eds, Pergamon Press, vol.1, pp.247-253.
Sehitoglu H. and Karasek M., (1986). Journal of Engineering Materials and Technology, Transactions of ASME, vol.108, pp.192-198.
Taira S., (1973). Fatigue at Elevated Temperatures, ASTM STP 520, American Society for Testing Materials, pp.239-254.

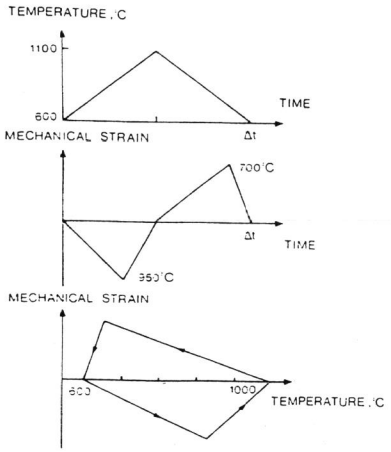

Fig.1. Shape of the thermal mechanical fatigue cycle : a) temperature versus time (Δt is the cycle period); b) mechanical strain versus time; c) mechanical strain versus temperature.

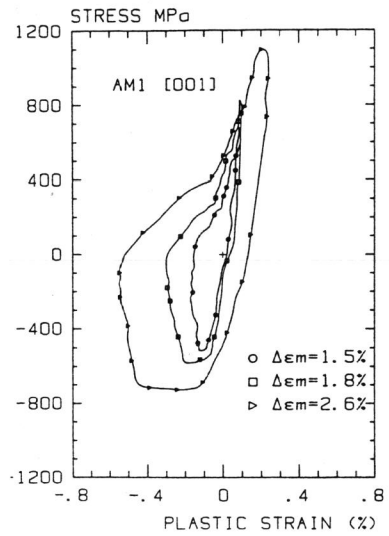

Fig.2. Stabilized stress - plastic strain loops under TMF cycling from 600°C to 1100°C for various mechanical strain ranges.

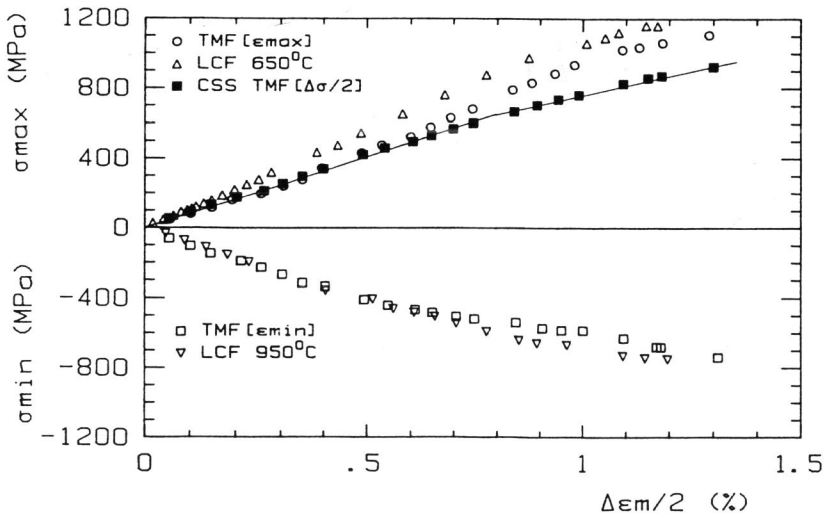

Fig.3. Cyclic stress-strain curves obtained under TMF and isothermal cycling.

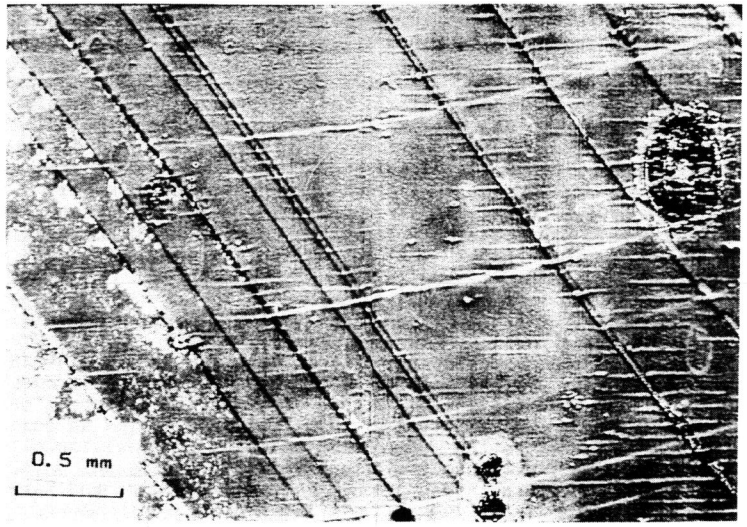

Fig.4. Scanning electron micrograph showing the surface of a TMF specimen ($\Delta\varepsilon_m$ = 2,6%)

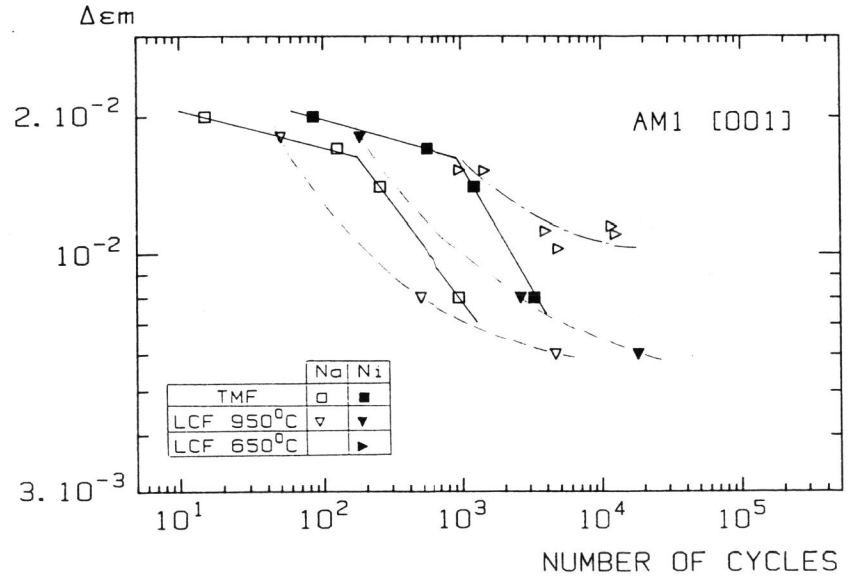

Fig.5 Variation of the number of cycles to 50μm and 0.3mm crack depth with the mechanical strain range under TMF cycling and LCF cycling at 650°C and 950°C.

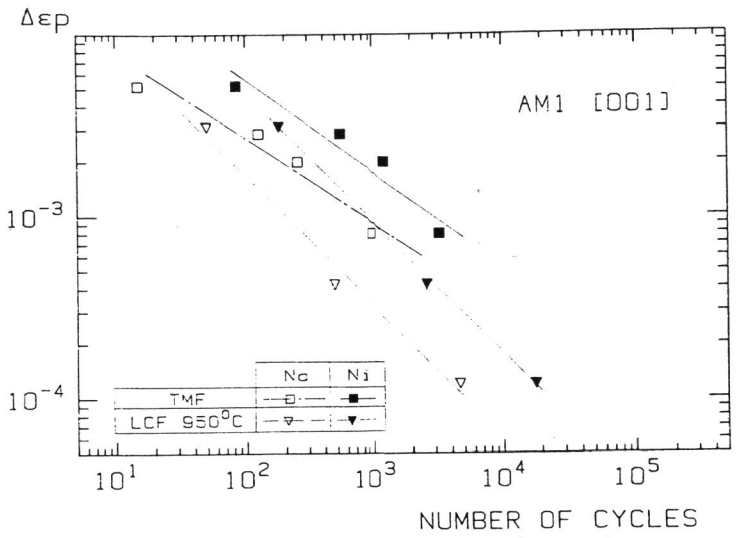

Fig.6. Comparison of the number of cycles to 50μm and 0.3 mm crack depth versus the plastic strain range under TMF cycling and LCF cycling at 950°C.

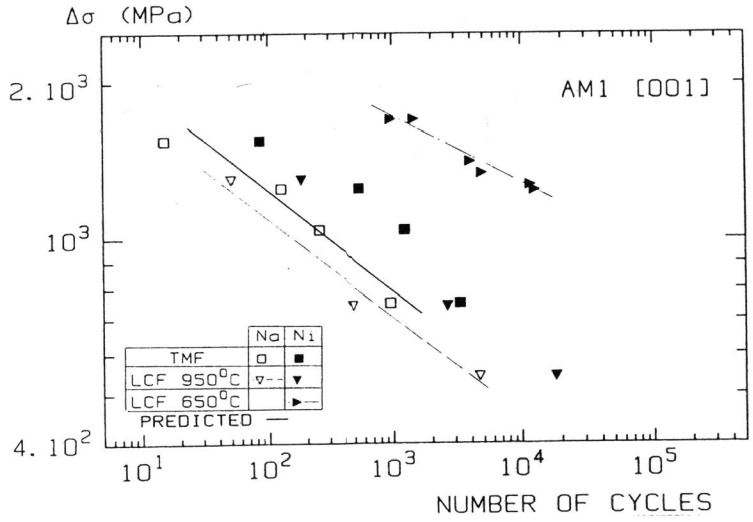

Fig.7. Variation of the number of cycles to 50μm and 0.3 mm crack depth with the stress range under TMF cycling and LCF cycling at 650°C and 950°C : Comparison between predicted TMF life to crack initiation (solid line) from Eq.1 and experimental data to a 50μm crack depth.